



## Full Text View

[Volume 29, Issue 6 \(June 1999\)](#)

### Journal of Physical Oceanography

 Article: pp. 1382–1391 | [Abstract](#) | [PDF \(424K\)](#)

## Intrusions: What Drives Them?

**Dave Hebert**

*Graduate School of Oceanography, University of Rhode Island, Narragansett, Rhode Island*

(Manuscript received November 7, 1997, in final form November 30, 1998)

DOI: 10.1175/1520-0485(1999)029<1382:IWDT>2.0.CO;2

### ABSTRACT

The driving mechanism for the observed interleaving of water masses is generally assumed to be double-diffusive mixing. However, some observations of intrusions have been made in regions where the mean stratification is stable to double-diffusive mixing. It has been hypothesized that a finite amplitude disturbance must occur to produce regions where the stratification allows double-diffusive mixing or that an instability due to differences in the molecular diffusivity of salinity and temperature produces the desired stratification for double-diffusive mixing to start. There is also the possibility of a differential vertical flux of salt and heat due to incomplete mixing by turbulence. The basis of this idea is described in this paper. Growth rates, vertical scales, and cross-frontal slopes of intrusions predicted by this process are compared to those predicted by double-diffusive mixing.

### 1. Introduction

In most frontal regions where water masses with contrasting temperature and salinity properties meet laterally, an interleaving of the different water masses has been generally observed. These features are commonly referred to as intrusions. From shelf-break fronts ([Horne 1978](#)) to the Antarctic Circumpolar Current ([Joyce et al. 1978](#)), the observation of intrusions has been taken as evidence for strong lateral mixing. [Hebert et al. \(1990\)](#) observed changes in a Mediterranean salt lens drifting in the Canary Basin over a two-year period and concluded that intrusive mixing was the primary mechanism for its decay. Other than that experiment, lateral mixing rates by intrusions have been only speculated. [Ruddick and Hebert \(1988\)](#) estimated that the cross-frontal velocities are on the order of several millimeters per second—making it almost impossible to determine cross-frontal fluxes of salt, heat, and mass directly. Thus, to determine the lateral mixing rates of intrusions and how to parameterize them, it is important to determine the dynamics driving the intrusions and the resulting cross-frontal fluxes.

The driving mechanism for the cross-frontal velocity of the intrusions (i.e., the horizontal pressure gradients) is due to divergences in vertical density fluxes, generally assumed to be due to double-diffusive mixing and mainly by salt fingering. Most of the theoretical studies to date have looked at the initial growth of the intrusions using linear stability analysis with parameterizations of the vertical flux by salt fingers ([Stern 1967](#); [Toole and Georgi 1981](#); [McDougall 1985](#); [Walsh and Ruddick 1995](#)). These studies can predict the growth rate, vertical scale, and slopes of the fastest growing mode (i.e., the intrusions). In these studies, it is assumed that basic background salinity and temperature structure is favorable to salt fingering and the intrusions are small perturbations to this stratification. Thus, the vertical fluxes are only due to salt fingers.

#### Table of Contents:

- [Introduction](#)
- [Turbulent mixing](#)
- [Stability analysis](#)
- [Discussion](#)
- [REFERENCES](#)
- [APPENDIX](#)
- [FIGURES](#)

#### Options:

- [Create Reference](#)
- [Email this Article](#)
- [Add to MyArchive](#)
- [Search AMS Glossary](#)

#### Search CrossRef for:

- [Articles Citing This Article](#)





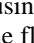
#### Search Google Scholar for:

- [Dave Hebert](#)

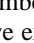

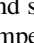
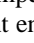
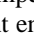
However, [Holyer \(1983\)](#) examined the situation before salt fingers have formed and found that the difference in molecular diffusivity for salt and heat could be responsible for an initial instability. She found that this perturbation could grow even for regimes where the stratification is stable both in temperature and salinity. Her conclusion was that this resulting growing instability, which had a much smaller vertical scale than the observed intrusions in the ocean, could be responsible for producing salt fingering and diffusive interfaces upon which double-diffusive mixing would then drive the intrusions.

In this paper, a third mixing process is proposed to drive the intrusions—incomplete turbulent mixing. This idea is analogous to Holyer's except that eddy fluxes replace molecular fluxes on the subintrusion scales. A linear stability analysis is performed for unequal salt and heat fluxes by turbulent mixing. Two possible parameterizations of this mixing process are examined. The first is using a flux ratio parameterization, as done for the double-diffusive mixing studies (e.g., [Toole and Georgi 1978](#)). The second is an eddy diffusivity ratio parameterization similar to that used by [Holyer \(1983\)](#). The results of this parameterization will be similar to that found by Holyer except the scaling used will be more consistent with that used in previous double-diffusive studies (e.g., [Toole and Georgi 1981](#); [McDougall 1985](#); [Walsh and Ruddick 1995](#)). However, a slightly different scaling will be used here to allow an easy comparison of growth rates, vertical scales, and cross-frontal slopes of intrusions driven by salt-finger mixing with those driven by diffusive-convection mixing and turbulent mixing.

## 2. Turbulent mixing

Our concept of turbulent mixing in the ocean, especially in the context of eddy diffusivities, is based on theories of high Reynolds number, homogeneous, isotropic turbulence with scalars that are passive (i.e., not affecting the dynamics of the flow). In the stratified (anisotropic) interior of the ocean where turbulence is of moderate-to-low Reynolds number and intermittent, the application of the same diffusivity coefficient for heat and salt is questionable. As an example of this, imagine the simple case of a two-layer fluid in which a turbulent eddy entrains some water from the lower layer into the upper layer ([Fig. 1a](#) ). As this water parcel is stirred by the turbulence in the upper layer, the salt and heat anomaly diffuse at different rates by molecular processes since the molecular diffusivity for temperature is approximately 100 times larger than that for salt. However, with continuous turbulence, the turbulent motions continue to stir the water parcel into the upper layer ([Fig. 1b](#) ) until all of the anomaly of heat and salt of the water parcel has diffused. This is the basis for our classic idea that salinity ( $S$ ) and temperature ( $T$ ) should have the same eddy diffusivity in the ocean. The flux of heat and salt are proportional to their difference between the two layers. However, imagine that some time after the water parcel is entrained into the upper layer ([Fig. 1b](#) ), the turbulence decays and the turbulent velocities can no longer keep the water parcel entrained in the upper layer. While the turbulence was active, the water parcel was stirred into the upper layer and more heat was diffusing than salt ([Fig. 1b](#) ). If the turbulence stops and the water parcel has not been completely mixed, it would sink and the fluid restratify ([Fig. 1c](#) ). Now, proportionally more heat has been transferred vertically than salt compared to their difference between the two layers. Thus, the eddy diffusivity for temperature would be greater than that for salt.

There is some evidence of the differential transport of salt and heat by turbulent mixing from laboratory experiments. In a two-layer grid-stirring experiment similar to that described above, [Turner \(1968\)](#) found that the transport efficiency of turbulence forced by the grid could depend on the property ( $T$  or  $S$ ) that was being used to produce the original density difference between the two layers. For large enough layer Richardson numbers, the entrainment velocity for the temperature-stratified case was greater than that found for the salt-stratified case. [Altman and Gargett \(1987\)](#) examined the same laboratory experiment with both temperature and salt stratification present at the same time. They confirmed Turner's result that the temperature entrainment rate was greater than the salt entrainment. In a laboratory stratified shear flow, [Sullivan and List \(1994\)](#) found that the entrainment varied greatly with the layer Richardson number and Péclet number (which will be different for temperature and salt under the same flow regime). In different regions of this parameter space, different mixing processes (e.g., Kelvin-Helmholtz instability, wave breaking) dominate the mixing and affect the entrainment rates.

It is not clear how to apply these results of continuously forced, low Reynolds number turbulent processes to intermittent, higher Reynolds number turbulent mixing processes in the ocean. Based on laboratory experiments, such as [De Silva and Fernando \(1992\)](#), we expect that a shear instability starts at a particular location ([Fig. 2a](#) ) and grows into an overturning billow ([Fig. 2b](#) ). This gravitationally unstable billow generates turbulent motions that result in a chaotic pattern of small-scale temperature and salinity fluctuations ([Fig. 2c](#) ). During this whole period, molecular diffusion is attempting to remove the large temperature and salinity gradients generated by the stirring motions of the turbulence. If the turbulence is strong and persistent enough, the mixing patch will be homogenized ([Fig. 2d](#) ). However, if the turbulence stops before this time, the water in the mixing patch (e.g., [Fig. 2c](#) ) would restratify. During the turbulent mixing and restratification processes, molecular diffusion is removing both the salinity and temperature fluctuations. The relative timescale of the molecular diffusion rate to the turbulent mixing and restratification rates would determine whether the effective diffusivities of salt and heat are equal. Very long turbulent mixing and/or restratification timescales would allow both the salinity and temperature anomalies to completely diffuse away, resulting in the same effective eddy diffusivities for temperature and salinity. Shorter turbulent mixing and restratification timescales would produce a larger effective eddy diffusivity for temperature than for salinity. However, it is not clear how the eddy diffusivities would depend on these timescales or what is exactly meant by a very long timescale for turbulent mixing and restratification. The timescale for turbulent mixing in the ocean is generally believed to be on the order of several hours. The timescale to remove a temperature anomaly with length scale  $L$  is  $L^2/\kappa_T$ , where  $\kappa_T$  is the molecular diffusivity for temperature. For  $L = 1$  m, the timescale is on the order of 100 days. For salinity, the timescale is 100 times longer. The timescale for the restratification of a mixing patch is unknown but could be as long as several days ([Sun et al. 1996](#)). Even if the restratification process is this long, it is not clear whether the effective diffusivity of temperature and salinity would be the same. During the restratification process, the density fluctuations generated by the turbulent motions would diffuse more heat than salt while restratifying. The distribution of the

temperature and salinity fluctuations in the mixing patch would probably affect the effective diffusivities of temperature and salinity.

It is likely that the turbulent mixing processes in the ocean are not persistent enough to homogenize a mixing patch. Observations of turbulent patches in the ocean (e.g., [Dillon 1982](#)) show that most of the mixing patches are similar to that shown in [Fig. 2c](#). For most observed patches, the density profile, after being reordered to make a gravitationally stable profile, is not significantly different from the believed initial state. Thus, the mixing patch has not been completely homogenized. This is weak evidence that some restratification must be occurring. In fact, this is the basis of [Gibson's \(1982\)](#) fossil turbulence idea—the presence of temperature fluctuations does not guarantee that active mixing is presently occurring.

Unlike the double-diffusive mixing studies, it is not clear how to parameterize the differential turbulent transport of heat and salt. Thus, two possible parameterizations are examined. The first is the same as that used for the double-diffusive mixing case. The salinity flux is parameterized in terms of a constant diffusivity and the temperature flux is proportional to the salt flux (i.e., a flux ratio parameterization). The other parameterization uses constant, but unequal, eddy diffusivity coefficients for salt and heat (i.e., a diffusivity ratio parameterization). We will examine the linear stability of both scenarios.

### 3. Stability analysis

We will obtain intrusion properties (e.g., cross- and alongfrontal slopes, vertical length scales, and growth rates) of the fastest growing instability mode. This stability analysis is the same as that done by [Toole and Georgi \(1981\)](#) and [McDougall \(1985\)](#) for intrusions driven by salt-finger mixing. However, a slightly different scaling will be used. Although this scaling does not reduce the solutions to a form as compact (i.e., fewer independent variables) as that used by Toole and Georgi, this different scaling has two advantages. First, it allows the dependence of the intrusion slope, vertical scale, and growth rate on the ratio of the flux of temperature to that of salinity expressed in terms of density ( $\gamma$  as defined later) and the strength of double-diffusion activity (e.g., the vertical effective diffusivity of salt  $K_S$ ), both a function of  $R_\rho$  (which is defined later), to be viewed more easily. For the stability analysis, the flux ratio and effective diffusivity are assumed constant. In other words, the perturbations of salinity and temperature are small compared to the mean values. However, it is known that the flux ratio and effective diffusivity quantities change with  $R_\rho$  ([Turner 1973](#)). While their functional dependency on  $R_\rho$  is not known, their general tendencies are. In the compact scaling of [Toole and Georgi \(1981\)](#), the tendency of their unsealed quantities, such as the growth rate, with  $R_\rho$  is not known, thus making it difficult to ascertain what happens when  $R_\rho$  changes. Second, the Toole and Georgi scaling does not reduce the number of independent variables for the case where the vertical fluxes of salt and heat are parameterized in terms of eddy diffusivities, as discussed later.

The basic background state for the stability analysis consists of a fluid at rest with constant vertical gradients of temperature  $T$  and salinity  $S$  and constant horizontal gradients of salinity and temperature in the  $x$  direction. There are no mean gradients in the  $y$  direction. The horizontal gradients of salinity and temperature are chosen such that isopycnals are horizontal. That is,

$$\alpha \frac{\partial \bar{T}}{\partial x} = \beta \frac{\partial \bar{S}}{\partial x}, \quad (1)$$

where  $\alpha$  and  $\beta$  are the thermal expansion and haline contraction coefficients of seawater. The overbars represent the basic state. A linear equation of state is assumed. As in the previous studies ([Toole and Georgi 1981](#); [McDougall 1985](#)), the conservation equations used in the linear stability analysis are

$$\frac{\partial u'}{\partial t} - f v' = -\frac{1}{\rho_0} \frac{\partial p'}{\partial x} + A \frac{\partial^2 u'}{\partial z^2} \quad (2)$$

$$\frac{\partial v'}{\partial t} + f u' = -\frac{1}{\rho_0} \frac{\partial p'}{\partial y} + A \frac{\partial^2 v'}{\partial z^2} \quad (3)$$

$$\frac{\partial w'}{\partial t} = -\frac{1}{\rho_0} \frac{\partial p'}{\partial z} + g(\alpha T' - \beta S') + A \frac{\partial^2 w'}{\partial z^2} \quad (4)$$

$$\frac{\partial x}{\partial t} + \frac{\partial y}{\partial t} + \frac{\partial z}{\partial t} = 0, \quad (7)$$

where  $A$  is the constant vertical eddy viscosity (viscous terms in the horizontal directions are assumed negligible) and primed quantities are the perturbation (i.e., intrusion) components. The vertical fluxes of salinity and temperature are represented by  $F^S$  and  $F^T$ . As in [Toole and Georgi \(1981\)](#) and [McDougall \(1985\)](#), divergences of the vertical fluxes are assumed to be more important than the horizontal fluxes. The actual form of the vertical fluxes will depend on the mixing process that is parameterized as described below.

For both the flux ratio and diffusivity ratio parameterizations, the vertical flux of salinity is parameterized as

$$F^S = -K_S \frac{\partial S}{\partial z}, \quad (8)$$

where  $K_S$ , the effective diffusivity for salinity, is assumed to be constant for the stability analysis. This assumption has been used for the previous double-diffusively driven intrusion studies. For the flux ratio parameterization, the vertical temperature flux is represented as

$$F^T = -\gamma \left( \frac{\beta}{\alpha} \right) K_S \frac{\partial S}{\partial z}, \quad (9)$$

where the flux ratio

$$\gamma = \frac{\alpha F^T}{\beta F^S}. \quad (10)$$

For salt-finger mixing,  $\gamma < 1$ . In their stability studies, [Toole and Georgi \(1981\)](#) and [McDougall \(1985\)](#) assumed that both  $K_S$  and  $\gamma$  were constant. This assumption limits their intrusion solutions to small perturbations of the mean salinity and temperature gradients such that  $K_S$  and  $\gamma$  do not change significantly. [Walsh and Ruddick \(1995\)](#) examined the case where  $K_S$  varied with density ratio

$$R_\rho = \left( \alpha \frac{\partial T}{\partial z} \right) / \left( \beta \frac{\partial S}{\partial z} \right), \quad (11)$$

but  $\gamma$  remained a constant. The density ratio provides a measure of the strength of double-diffusive activity. For the salt-finger regime, the vertical stratification is such that warm salty water overlies cooler fresher water (i.e.,  $R_\rho > 1$ ). With respect to the salinity distribution only, the water column would be gravitationally unstable. However, the temperature gradient is sufficient to keep the water column gravitationally stable. As  $R_\rho \rightarrow 1$ , the salt-finger activity increases. That is, for the same vertical salinity gradient, the flux of salt increases. In other words,  $K_S$  increases as  $R_\rho \rightarrow 1$ .

For the diffusive–convection region, the same definitions for  $R_\rho$  and  $\gamma$  will be used instead of the standard definitions for diffusive–convection studies that are the inverse of the salt-fingering-based definitions. For the diffusive–convection regime, cool fresh water overlies warmer saltier water (i.e.,  $0 < R_\rho < 1$ ). The water column is gravitationally unstable in terms of the temperature distribution only. The vertical flux of temperature (in terms of density) is greater than that for salinity (i.e.,  $\gamma > 1$ ). Double-diffusive activity increases as  $R_\rho \rightarrow 1$ . The solutions found by [Toole and Georgi \(1981\)](#), [McDougall \(1985\)](#), and [Walsh and Ruddick \(1995\)](#) and below for the salt-fingering regime can be applied to the diffusive–convection regime with the appropriate transformation of variables—see [Walsh and Ruddick \(1995\)](#) for the details. However, in this paper, the same scaling will be used for all regimes in order to allow easy comparisons.

For the turbulent mixing case, unlike the double-diffusive case, there is no restriction on whether stratification is gravitationally unstable in salinity or temperature. However, based on the discussion of the differential transport of heat and salt by incomplete turbulent mixing, we expect  $\gamma > 1$ .

For turbulent mixing, the differential flux of salt and heat could also be parameterized in terms of constant eddy diffusivity coefficients for salinity and temperature. The eddy diffusivity coefficient for heat,  $K_T$ , can be expressed as a factor of the salt diffusivity coefficient. That is,

$$F^T = -K_T \frac{\partial T}{\partial z} = -\Gamma K_S \frac{\partial T}{\partial z},$$

where

$$\Gamma = \frac{K_T}{K_S} > 1$$

for our incomplete turbulent mixing process.

For the stability analysis, wavelike solutions of the form

$$\begin{aligned} & \{u', v', w', p', S', T'\} \\ & = \{U_0, V_0, W_0, P_0, S_0, T_0\} \exp[\lambda t + i(kx + ly + mz)] \end{aligned}$$

are assumed for the fastest growing instability mode. Substituting these solutions into the conservation equations, (2)–(7), gives the characteristic equation for the growth rate  $\lambda$ .

As found by [McDougall \(1985\)](#), for the fastest growing mode, the alongfrontal slope  $l/m$  of the intrusions is simply related to the cross-frontal slope,  $s = k/m$ , by

$$\frac{l}{m} = \frac{f}{(\lambda + Am^2)} \frac{k}{m}. \quad (12)$$

After substituting this relationship into the characteristic equation, it is found that the fastest growing modes are independent of the Coriolis force and the alongfrontal intrusion slope. Eliminating one of the solutions to the simplified characteristic equation (a decaying mode) and assuming that the cross-frontal slope of the intrusion is small (i.e.,  $s \ll 1$ ), the characteristic equation for the diffusivity ratio parameterization becomes

$$\begin{aligned} & \left(\frac{\lambda}{N\Sigma}\right)^3 + \left[ \frac{m^2}{N\Sigma/K_S}(1 + \sigma) + \frac{m^2}{N\Sigma/K_S}\Gamma \right] \left(\frac{\lambda}{N\Sigma}\right)^2 \\ & + \left[ \left(\frac{m^2}{N\Sigma/K_S}\right)^2 \sigma + \left(\frac{s}{\Sigma}\right)^2 + \frac{\left(\frac{m^2}{N\Sigma/K_S}\right)^2 \Gamma(1 + \sigma)}{N\Sigma} \right] \frac{\lambda}{N\Sigma} \\ & + \left[ \frac{m^2}{N\Sigma/K_S} \left(\frac{s}{\Sigma}\right)^2 \frac{1}{(R_\rho - 1)} \left( (R_\rho - \Gamma) - (1 - \Gamma) \frac{\Sigma}{s} \right) \right. \\ & \left. + \left(\frac{m^2}{N\Sigma/K_S}\right)^3 \Gamma \sigma \right] = 0, \quad (13) \end{aligned}$$



with  $\Sigma = (\partial\bar{S}/\partial x)/(\partial\bar{S}/\partial z)$ , which is related to the slope of the mean isohalines [i.e.,  $-(\partial z/\partial x)_{\bar{S}}$ ], and the Prandtl number,  $\sigma = A/K_S$ . The characteristic equation for the flux ratio parameterization found by [Toole and Georgi \(1981\)](#) and [McDougall \(1985\)](#) is the same as (13) but without the underlined terms and with  $\gamma$ , the flux ratio, replacing  $\Gamma$ , the diffusivity ratio. Equation (13) is expressed in a nondimensional form. The slope of the intrusions is scaled by the slope of the mean isohalines. The growth rate of the intrusions  $\lambda$  is scaled by the product of the buoyancy frequency and the slope of the mean isohalines. The vertical length scale of the intrusions is nondimensionalized by a vertical scale, which represents the vertical scale of a salinity fluctuation that would diffuse away in the timescale used for growth rate of the intrusion.

Two additional equations,  $\partial\lambda/\partial s = \partial\lambda/\partial m = 0$  (additional conditions for determining the fastest growing modes with respect to cross-frontal slope and vertical scale), are obtained by differentiating the characteristic equation with respect to  $s$  and  $m$ . After some manipulation, we have solutions for the nondimensional cross-frontal slope,  $s/\Sigma$ , vertical wavenumber,  $m/(N\Sigma/K_S)^{1/2}$ , and growth rate,  $\lambda/(N\Sigma)$ , of the fastest growing intrusions. (See the appendix for the details.)

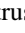
The cross-frontal slope, vertical scale, and growth rate of the fastest growing intrusion depends on the Prandtl number  $\sigma$ , the density ratio  $R_\rho$ , and the flux ratio  $\gamma$  or diffusivity ratio  $\Gamma$ , depending on how the vertical mixing is parameterized. To illustrate this parameter dependence, a couple of examples are given for different stratification regimes and  $\sigma = 1$  ([Figs. 3](#) and [4](#)). Since the dependence of the strength of doubled-diffusive mixing on  $R_\rho$  is complex, the Turner angle,

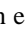

$$Tu = \tan^{-1} \left( \frac{R_\rho + 1}{R_\rho - 1} \right),$$

([Ruddick 1983](#)) is used in the figures instead of  $R_\rho$ . Turner angles between  $45^\circ$  and  $90^\circ$  represent the salt-fingering regime, with the strongest activity near  $90^\circ$ . Likewise, Turner angles between  $-45^\circ$  and  $-90^\circ$  represent the diffusive-convection regime, with the strongest activity near  $-90^\circ$ . Turner angles between  $-45^\circ$  and  $45^\circ$  represent regions where the stratification is stable in both  $T$  and  $S$ .

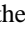
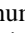
For the salt-fingering regime ( $Tu > 45^\circ$ ,  $\gamma < 1$ ), the growth rate, vertical wavenumber and cross-frontal slope of the intrusions increase as the salt-fingering activity increases (i.e.,  $Tu \rightarrow 90^\circ$ ) ([Fig. 3](#) ). For a constant Turner angle, as the flux ratio,  $\gamma = (aF_T)/(\beta F_S)$ , decreases, the growth rate, vertical wavenumber, and cross-frontal slope increases. Similar results are found in the diffusive-convection regime ( $Tu < -45^\circ$ ,  $\gamma > 1$ ). Increased double-diffusive convection occurs as  $Tu \rightarrow -90^\circ$ . Faster growing, thicker, and more steeply sloped intrusions occur for the more diffusively unstable regime ([Fig. 3](#) ). These dependences of the intrusion properties for the diffusive-convection regime are not the mirror image of that found for the salt-fingering regime as we might have expected. The reason for the different appearance is the scaling of the intrusion properties by  $\Sigma$ , which depends on the slope of the isohalines. For the transformation of the diffusive-convection regime to mimic the salt-fingering regime, the intrusion properties should be scaled by the isotherm slopes. The ratio of isotherm slopes to isohaline slopes has a Turner angle dependence.

The dependence of the growth rate, vertical scale, and slope of the intrusions on the Turner angle and flux ratio simply illustrate that the larger the buoyancy flux available to drive the intrusions, the faster they will grow, the more steeply they are tilted, and the larger the vertical scale that can grow. The dependence of the properties of the fastest growing intrusion on the Prandtl number (not shown) is as expected. The smaller the Prandtl number (the weaker the friction), the faster the intrusions grow and the smaller the vertical scale of the fastest growing mode.

As evident in [Fig. 3](#) , there are stratification and flux ratio regimes where intrusions can grow; yet these regions are where double-diffusive mixing does not occur. Interestingly, there are growing intrusions for regions where the stratification is stable both in temperature and salinity (i.e.,  $-45^\circ < Tu < 45^\circ$ ). Thus, it is possible to have intrusions grow in a region where double-diffusive mixing does not occur. There is some weak observational evidence confirming this possibility. [Ruddick \(1992\)](#) observed intrusions in a region of a Mediterranean salt lens that had an overall stable stratification to double diffusion.

One possible explanation is that incomplete turbulent mixing (described earlier) could be active. This process can be active for all stratification regimes shown, and with  $\gamma > 1$ . In the salt-fingering regime, there is only a limited range of  $R_\rho$  (or Turner angles) and flux ratios where the turbulently driven growing intrusions can exist ([Fig. 3](#) ). As this boundary is approached, the cross-frontal slope of the intrusions increases rapidly. [Our assumption of  $s \ll 1$  for the characteristic [equation \(13\)](#) is not violated in this region if  $\Sigma \ll 1$ .] This boundary is  $\gamma = R_\rho$ . It should also be noted that the cross-frontal slope of the intrusions in this regime is the opposite to that found for salt-finger-driven intrusions. In the region of salt fingering, the turbulently driven intrusions have a faster growth rate for the same buoyancy flux ([Fig. 5](#) ). However, since we do not know the flux ratio (or buoyancy flux) for incomplete turbulent mixing, we cannot determine whether turbulently driven intrusions will grow faster than salt-finger-driven intrusions for the same stratification (i.e.,  $R_\rho$ ).

Above, the vertical flux of temperature was parameterized as proportional to the salinity flux. However, it is not clear whether this parameterization is appropriate. Perhaps, the eddy diffusivity of temperature should be parameterized as proportional to the diffusivity of salinity. [Gargett and Holloway \(1992\)](#) used this type of parameterization in their global circulation model studies.

The dependence of the intrusion cross-frontal slope and growth rates for the fastest growing mode on the Turner angle, Prandtl number, and diffusivity ratio (e.g., [Fig. 4](#) ) is similar to that found for the fastest growing mode using the flux ratio parameterization ([Fig. 3](#) ). However, the dependence of the vertical wavenumber is different, especially for small Prandtl numbers (not shown) and the vertical wavenumber is smaller for the diffusivity ratio parameterization.

#### 4. Discussion

In attempting to determine the driving mechanism for intrusions, two properties of observed intrusions are often compared to predictions made by linear stability analysis. These are the vertical scale of the intrusions and the cross-frontal slope. In the study of [Toole and Georgi \(1981\)](#), they compared their results to five datasets. However, as pointed out by [McDougall \(1985\)](#), these datasets are not appropriate since the basic stratification was not salt fingering favorable—an assumption in their linear stability analysis. For regions where the basic stratification is salt fingering favorable, the direction of the cross-frontal slope is often used to validate the assumption that salt-finger fluxes are responsible for driving the intrusions. However, as shown by [Toole and Georgi \(1981\)](#) and [McDougall \(1985\)](#), the alongfrontal slope of the fastest growing intrusion is generally larger than the cross-frontal slope. Thus, if a cross-frontal CTD transect is not truly cross-frontal but at a slight angle to the front, the observed slope of the intrusions may be due to the alongfrontal slope. We have shown above that intrusions driven by turbulent mixing can occur in salt-fingering favorable conditions, have approximately the same vertical scale as intrusions driven by salt fingers, and can grow at a faster rate. The only observable difference is the direction of cross-frontal slope and, as mentioned above, this can be difficult to determine in the field.

In order to assess the importance of turbulent mixing in driving intrusions, it is necessary to determine how to parameterize the vertical flux of salt and heat. Should a flux ratio or differential diffusivities of heat and salt be used? And, what should be the values of these parameters? For the case of differential diffusivities, constraints can be placed on the ratio of the diffusivity of temperature to salinity. For complete turbulent mixing, a lower limit of 1 is set. Without any turbulent mixing, molecular diffusivities set the upper limit of approximately 100. In their study of the effectiveness of differential diffusivities of heat and salt, [Gargett and Holloway \(1992\)](#) used a diffusivity coefficient ratio of 2. To address this aspect of the problem, laboratory experiments simulating mixing processes as intermittent internal wave breaking must be done.

Finally, the vertical size of the intrusions must be greater than size of the subintrusion mixing processes. The vertical scale of oceanic intrusions are usually several meters to tens of meters. The vertical scale of the salt-fingering regions and double-diffusive regions in oceanic intrusions are usually on the order of tens of centimeters to a couple of meters. The vertical scale of a turbulent mixing patch is approximately the Ozmidov scale,  $L_O = (\epsilon/N^3)^{1/2}$ , where  $\epsilon$  is the turbulent kinetic energy dissipation rate and  $N$  is the buoyancy frequency. Most turbulent patches have vertical scales less than a few meters (e.g., [Dillon 1982](#); [Moum 1996](#)).

Almost all of the linear stability analyses have been based on simple parameterizations of the vertical fluxes of salt and heat. [Walsh and Ruddick \(1995\)](#) extended the work of [Toole and Georgi \(1981\)](#) by using a diffusivity coefficient for salinity that was a function of  $R_\rho$ . They showed that the growth rates were larger for this variable diffusivity compared to the constant coefficient case. The observations of salinity and temperature fields in intrusions are definitely beyond the small perturbations assumed in the linear stability analysis. Even if turbulent mixing were not important, the salinity and temperature gradients are such that salt-finger mixing would be occurring on one interface and diffusive-convection mixing would be occurring on the other interface of an intrusion. To really understand the dynamics of finite amplitude intrusions, it is necessary to use more realistic parameterizations of vertical mixing which depend on the present conditions. [Walsh and Ruddick \(1998\)](#) have started research on this topic with a one-dimensional model of finite amplitude intrusions.

#### Acknowledgments

I thank Dan Kelley, Brian May, Barry Ruddick, and Dave Walsh for the many discussions we had on the dynamics of intrusions. Brian May pointed out the weakness of using the cross-frontal slope of intrusions as a test for determining the driving mechanism of intrusions. I thank the reviewers for their valuable comments, which improved this work and Dr. Nelson Hogg for his superb job as editor. This work has been supported by the Office of Naval Research, Grants N00014-94-1-0476 and N00014-96-1-0618.

---

#### REFERENCES

- Altman, D. B., and A. E. Gargett, 1987: Differential property transport due to incomplete mixing in a stratified fluid. *Proc. Third Int. Symp. on Stratified Flows*, Pasadena, CA, California Institute of Technology..
- De Silva, I. P. D., and H. J. S. Fernando, 1992: Some aspects of mixing in a stratified turbulent patch. *J. Fluid Mech.*, **240**, 601–625..
- Dillon, T. M., 1982: Vertical overturns: A comparison of Thorpe and Ozmidov length scales. *J. Geophys. Res.*, **87**, 9601–9613..
- Gargett, A. E., and G. Holloway, 1992: Sensitivity of the GFDL ocean model to different diffusivities for heat and salt. *J. Phys. Oceanogr.*, **22**, 1158–1177.. [Find this article online](#)
- Gibson, C. H., 1982: Alternative interpretation for microstructure patches in the thermocline. *J. Phys. Oceanogr.*, **12**, 374–383. [Find this article online](#)
- Hebert, D., N. Oakey, and B. Ruddick, 1990: Evolution of a Mediterranean salt lens: Scalar properties. *J. Phys. Oceanogr.*, **20**, 1468–1483.. [Find this article online](#)
- Holyer, J. Y., 1983: Double-diffusive interleaving due to horizontal gradients. *J. Fluid Mech.*, **137**, 347–362..
- Horne, E. P. W., 1978: Interleaving at the subsurface front in the slope water off Nova Scotia. *J. Geophys. Res.*, **83**, 3659–3671..
- Joyce, T. M., W. Zenk, and J. M. Toole, 1978: The anatomy of the Antarctic polar front in the Drake Passage. *J. Geophys. Res.*, **83**, 6093–6113..
- McDougall, T. J., 1985: Double-diffusive interleaving. Part I: Linear stability analysis. *J. Phys. Oceanogr.*, **15**, 1532–1541.. [Find this article online](#)
- Moum, J. N., 1996: Energy-containing scales of turbulence in the ocean thermocline. *J. Geophys. Res.*, **101**, 14 095–14 109..
- Ruddick, B., 1983: A practical indicator of the stability of the water column to double-diffusive activity. *Deep-Sea Res.*, **30**, 1105–1107..

- , 1992: Intrusive mixing in a Mediterranean salt lens—Intrusion slopes and dynamics mechanisms. *J. Phys. Oceanogr.*, **22**, 1274–1285.. [Find this article online](#)
- and D. Hebert, 1988: The mixing of Meddy “Sharon.” *Small-Scale Mixing in the Ocean*, J. C. J. Nihoul and B. M. Jamart, Eds., Elsevier Oceanography Series, Vol. 46, Elsevier, 249–262..
- Stern, M. E., 1967: Lateral mixing of water masses. *Deep-Sea Res.*, **14**, 747–753..
- Sullivan, G. D., and E. J. List, 1994: On mixing and transport at a sheared density interface. *J. Fluid Mech.*, **273**, 213–239..
- Sun, H., E. Kunze, and A. J. Williams III, 1996: Vertical heat-flux measurements from a neutrally buoyant float. *J. Phys. Oceanogr.*, **26**, 984–1001.. [Find this article online](#)
- Toole, J. M., and D. T. Georgi, 1981: On the dynamics and effects of double-diffusively driven intrusions. *Progress in Oceanography*, Vol. 10, Pergamon, 123–145..
- Turner, J. S., 1968: The influence of molecular diffusivity on turbulent entrainment across a density interface. *J. Fluid Mech.*, **33**, 639–656..
- , 1973: *Buoyancy Effects in Fluids*. Cambridge University Press, 368 pp..
- Walsh, D., and B. Ruddick, 1995: Double-diffusive interleaving: The influence of nonconstant diffusivities. *J. Phys. Oceanogr.*, **25**, 348–358.. [Find this article online](#)
- and —, 1998: Nonlinear equilibrium of thermohaline intrusions. *J. Phys. Oceanogr.*, **28**, 1043–1070.. [Find this article online](#)

## APPENDIX

### a. Flux ratio parameterization

The cross-frontal slope of the fastest growing mode is determined from the solution of

$$\begin{aligned} & \{4(R_\rho - \gamma)[(R_\rho - \gamma) - \sigma(R_\rho - 1)]\} \left(\frac{s}{\Sigma}\right)^3 - \{4(R_\rho - \gamma)[2(1 - \gamma) - (\sigma - 1)(R_\rho - 1)]\} \left(\frac{s}{\Sigma}\right)^2 \\ & + \{(1 - \gamma)[(4 - \sigma)(R_\rho - 1) + 5(1 - \gamma)]\} \left(\frac{s}{\Sigma}\right) - (1 - \gamma)^2 = 0. \end{aligned} \quad (\text{A1})$$

(Click the equation graphic to enlarge/reduce size)

The vertical wavenumber  $m$  and growth rate  $\lambda$  are given by

$$\left(\frac{m^2}{N\Sigma/K_S}\right)^2 = \left(\frac{s}{\Sigma}\right)^2 \left[ \frac{(1 - \gamma)\Sigma/s - (R_\rho - 1)}{(1 + \sigma)\delta^2 + 2\sigma\delta(R_\rho - 1)} \right] (R_\rho - 1) \quad (\text{A2})$$

and

$$\left(\frac{\lambda}{N\Sigma}\right) = \frac{\delta}{(R_\rho - 1)} \left(\frac{m^2}{N\Sigma/K_S}\right), \quad (\text{A3})$$

where

$$\delta = \left[ \frac{(1 - \gamma)\Sigma}{2s} - (R_\rho - \gamma) \right]. \quad (\text{A4})$$

### b. Diffusivity ratio parameterization

For the fastest growing mode,  $s/\Sigma$  must satisfy



$$\begin{aligned}
& + \langle -4(R_\rho - \Gamma)\{[2(1 - \sigma - \Gamma) + \sigma\Gamma]R_\rho^2 + [3(1 - \Gamma)^2 + \sigma(1 + \Gamma)]R_\rho + \sigma - 2\Gamma(1 + \sigma - \Gamma)\} \\
& - 4\sigma\Gamma(R_\rho - 1)^3\left(\frac{s}{\Sigma}\right)^3 + \{6(R_\rho - \Gamma)(1 - \Gamma)[(2 - \sigma - \Gamma)(R_\rho - 1) + 3(1 - \Gamma)]\}\left(\frac{s}{\Sigma}\right)^2 \\
& + \{(1 - \Gamma)^2[(\sigma + \Gamma - 6)(R_\rho - 1) - 7(1 - \Gamma)]\}\left(\frac{s}{\Sigma}\right) + (1 - \Gamma)^3 = 0.
\end{aligned} \tag{A5}$$

(Click the equation graphic to enlarge/reduce size)

The growth rate  $\lambda$  and vertical wavenumber  $m$  for this mode are

$$\left(\frac{\lambda}{N\Sigma}\right) = \frac{\delta}{(R_\rho - 1)}\left(\frac{m^2}{N\Sigma/K_s}\right) \tag{A6}$$

and

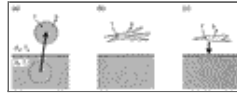
$$\left(\frac{m^2}{N\Sigma/K_s}\right)^2 = \left(\frac{s}{\Sigma}\right)^2 \left[ \frac{(1 - \Gamma)\Sigma/s - (R_\rho - \Gamma)}{(1 + \sigma + \Gamma)\delta^2 + 2(\sigma(1 + \Gamma) + \Gamma)(R_\rho - 1)\delta + 3\Gamma\sigma(R_\rho - 1)^2} \right] (R_\rho - 1), \tag{A7}$$

(Click the equation graphic to enlarge/reduce size)

where

$$\delta = \left( (1 - \Gamma)\frac{\Sigma}{2s} - (R_\rho - \Gamma) \right). \tag{A8}$$

## Figures



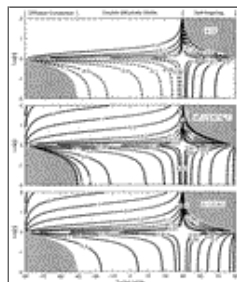
Click on thumbnail for full-sized image.

Fig. 1. Schematic of a turbulence entraining a patch of heavier water into the upper layer (a) and molecular diffusion of salt and heat occurring. Turbulence continues to strain the patch while its salinity and temperature anomaly decreases (b). If the turbulence stops, the patch, if not completely diffused away, will sink during the restratification process (c).



Click on thumbnail for full-sized image.

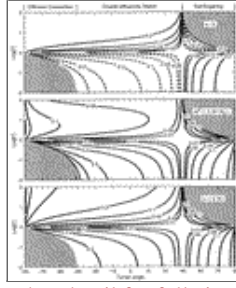
Fig. 2. Schematic of a growing shear instability (a), which becomes gravitationally unstable (b) and turbulence is generated (c). The contours represent isopycnals. Adjacent to each panel is an example of a vertical profile of density through the patch. In (d), it is assumed that the turbulence has stirred the patch long enough for molecular diffusion to remove the density fluctuations.



Click on thumbnail for full-sized image.

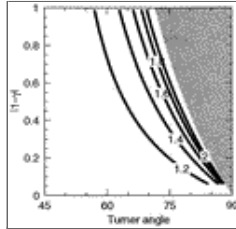
Fig. 3. The cross-frontal slope  $s$ , vertical wavenumber  $m$ , and growth rate  $\lambda$  of the fastest growing intrusion for a constant

Prandtl number ( $\sigma = 1$ ). [Contours of  $\pm 0.01$ ,  $\pm 0.02$ ,  $\pm 0.05$ ,  $\pm 0.1$ ,  $\pm 0.2$ ,  $\pm 0.5$ ,  $\pm 1$ ,  $\pm 2$ , and  $\pm 5$  are shown for  $s/\Sigma$ ,  $m^2/(N\Sigma/K_S)$ , and  $\lambda/(N\Sigma)$ .] Shaded areas show regions in which intrusions cannot grow.



[Click on thumbnail for full-sized image.](#)

Fig. 4. For a constant Prandtl number ( $\sigma = 1$ ), the cross-frontal slope  $s$ , vertical wavenumber  $m$ , and growth rate  $\lambda$  of the fastest growing intrusion for turbulent mixing assuming a diffusivity ratio  $\Gamma$  parameterization.



[Click on thumbnail for full-sized image.](#)

Fig. 5. The ratio of the growth rate of turbulently driven intrusions to the growth rate of salt-finger-driven intrusions as a function of buoyancy flux (proportional to  $|1 - \gamma|$  assuming the same effective diffusivity for salinity for both cases) and Turner angle.

Corresponding author address: Dr. Dave Hebert, Graduate School of Oceanography, University of Rhode Island, Narragansett, RI 02882-1197.

E-mail: [hebert@gso.uri.edu](mailto:hebert@gso.uri.edu)

[top](#) ▲



© 2008 American Meteorological Society [Privacy Policy and Disclaimer](#)  
Headquarters: 45 Beacon Street Boston, MA 02108-3693  
DC Office: 1120 G Street, NW, Suite 800 Washington DC, 20005-3826  
[amsinfo@ametsoc.org](mailto:amsinfo@ametsoc.org) Phone: 617-227-2425 Fax: 617-742-8718  
[Allen Press, Inc.](#) assists in the online publication of AMS journals.